Journal of Robotics and Control (JRC)
Volume 6, Issue 4, 2025
ISSN: 2715-5072, DOI: 10.18196/jrc.v6i4.25570

Adaptive Sliding Mode Control for Trajectory Tracking in Three-Wheeled Mobile Robots: Experimental Validation and Performance Analysis

Hoa Van Doan [1*]
[1] Faculty of Electrical Engineering - Automation, University of Economics – Technology for Industries, Ha Noi, Viet Nam
Email: [1] rvhoa@uneti.edu.vn
*Corresponding Author

***Abstract*—This paper presents an adaptive sliding mode control approach (ASMC) designed for trajectory tracking of a three-wheeled mobile robot (TWMR), accounting for external disturbances and wheel slippage effects. First, the TWMR system model is converted into a dynamic form of the tracking error, and then a SMC is designed for this error model. The synthetic disturbance is approximated through an adaptive law, which helps the system maintain high stability. The results from simulating the controller on Matlab/Simulink software, as well as implementing the algorithm on the experimental TWMR model, have demonstrated the accuracy and efficiency of the proposed method.**

Keywords—Trajectory Tracking; Three-Wheeled Mobile Robot; Adaptive Control; Sliding Mode Control; Disturbances; Wheel Slip.

I. INTRODUCTION

In the era of Industry 4.0, research and applications of robots in agriculture, services, especially in factories and enterprises, have become increasingly popular. Methods ranging from classical control [1]-[5] to modern control [6]-[19], model predictive control (MPC) [20]-[24], and intelligent control [25]-[42] have been proposed to improve the control quality of wheeled mobile robots (WMR). Previous studies often used a two-loop structure for WMR control design [43]-[50], which generally still meets system performance within acceptable limits. However, the use of two controllers—one for position tracking and another for velocity tracking—makes the system cumbersome and complex. Additionally, some dynamic control methods such as sliding mode control [51]-[57] and backstepping control [58]-[63] have been developed. When the dynamic equations contain uncertain parameters, authors have employed adaptive control [64]-[75], or combined adaptive control with fuzzy logic to approximate the unknown uncertainties [76]-[81], or integrated adaptive control with neural networks [82]-[85], achieving good control quality by compensating for model errors and system input noise. Most of these studies assume that WMR only experiences pure rolling without slipping. However, in practice, nonlinear factors such as friction and wheel slippage are incorporated into many models to improve the accuracy of robot operation [86]-[93], along with disturbances in kinematic and measurement models [94]-[97].

Some papers [1][5] present methods for designing Proportional-Integral-Derivative (PID) controllers with parameters that vary over time to enable the robot to automatically follow desired trajectories. Simulation results show that these controllers have simple structures and produce small errors during movement. However, these studies do not address issues related to dynamics, electromechanical interactions with the moving environment—such as Coulomb friction, payload, etc. Additionally, other works [25][26][28][30] propose methods for controlling autonomous robots along given trajectories based on fuzzy logic, with simulation results indicating stable motion and small errors even on relatively complex trajectories. However, in the study, the author only considered the kinematic model and ignored the impact of force on the robot's movement. The paper [64][65][86] presents an adaptive control method using a disturbance estimator, which is capable of compensating for the effects of wheel slip and external disturbances in both the kinematic and dynamic loops. However, the controller is still cumbersome, so the authors have proposed a structure using a parametric adaptive controller, in which a second-order fuzzy controller is used to compensate for disturbance uncertainty and wheel slip [87]. Some studies have considered input constraints to avoid providing too large a control torque at the initial moment to the motor [66][71][82]. However, the authors have not mentioned the wheel slip problem and the control structure is still complicated.

In practice, when WMR is active, wheel slippage often occurs when the Robot accelerates or escapes from a muddy area. The wheels start to slip and spin faster than the normal moving speed. This can lead to different consequences depending on whether the Robot is front-wheel drive or rear-wheel drive. Therefore, the aim of this paper is to propose a simple control structure consisting of only one control loop but still ensuring smooth and stable operation of TWMR. In addition, when designing the controller, the effects of external disturbances and wheel slippage affecting TWMR are still fully considered.

II. MODEL TRANSFORMATION OF THREE-WHEEL MOBILE ROBOT

A. Kinematic and Dynamic Modeling of Three-Wheel Mobile Robot

Imagine the setup where a TWMR is positioned within a stationary *OXY* coordinate system, while a local coordinate

system, denoted as *MX'Y'*, is attached to the robot, as illustrated in Fig. 1.

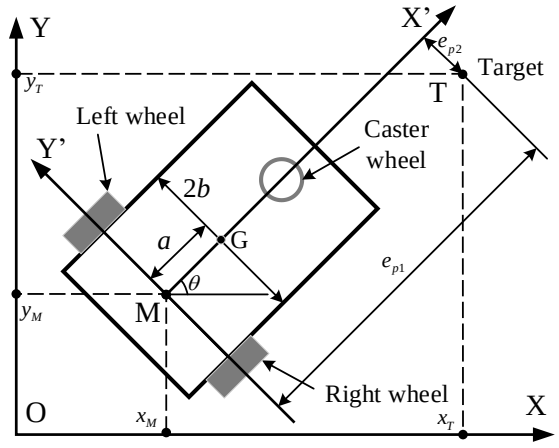

Fig. 1. Three-wheeled mobile robot model

Denote the angular velocities of the right and left wheel motors as $\dot{\varphi}_R$ and $\dot{\varphi}_L$; correspondingly, v_R and v_L represent the linear velocities of the right and left wheels. Based on Fig. 1, we obtain:

$$\begin{cases} v_R = r\dot{\varphi}_R \\ v_L = r\dot{\varphi}_L \end{cases} \tag{1}$$

In the presence of wheel slip, let μ_R and μ_L denote the axial slip ratios of the right and left wheels, respectively, while δ represents the slip of the wheel itself. The translational velocity β along the longitudinal axis perpendicular to the line connecting the two rear wheels and the actual angular velocity ϖ of the TWMR can then be determined using the following expressions [58]:

$$\beta = \frac{r(\dot{\varphi}_R + \dot{\varphi}_L)}{2} + \frac{\dot{\mu}_R + \dot{\mu}_L}{2} = \upsilon + \frac{\dot{\mu}_R + \dot{\mu}_L}{2} \tag{2}$$

$$\varpi = \frac{r(\dot{\varphi}_R - \dot{\varphi}_L)}{2b} + \frac{\dot{\mu}_R - \dot{\mu}_L}{2b} = \omega + \frac{\dot{\mu}_R - \dot{\mu}_L}{2b} \tag{3}$$

The dynamic equation describing the motion of the TWMR at its center of mass point G incorporates the influence of wheel slippage effects [1][58][84]:

$$\begin{cases} \dot{x}_G = \beta cos\theta - \dot{\delta} sin\theta - a\varpi sin\theta \\ \dot{y}_G = \beta sin\theta + \dot{\delta} cos\theta + a\varpi cos\theta \\ \dot{\theta} = \varpi \end{cases} \tag{4}$$

The non-holonomic constraint is [1][84]-[86]:

$$\begin{cases} \dot{\mu}_R = -r\dot{\varphi}_R + \dot{x}_G cos\theta + \dot{y}_G sin\theta + b\varpi \\ \dot{\mu}_L = -r\dot{\varphi}_L + \dot{x}_G cos\theta + \dot{y}_G sin\theta - b\varpi \\ \dot{\delta} = -\dot{x}_G sin\theta + \dot{y}_G cos\theta - a\dot{\theta} \end{cases} \tag{5}$$

Then the non-holonomic constraint condition is reduced to a vector form with the following general form:

$$A(\boldsymbol{q})\dot{\boldsymbol{q}} = 0 \tag{6}$$

where $\dot{\boldsymbol{q}} = \left[\dot{x}_G, \dot{y}_G, \dot{\theta}, \dot{\delta}, \dot{\mu}_R, \dot{\mu}_L, \dot{\varphi}_R, \dot{\varphi}_L\right]^T$

Combining (4) and (5) we have the equation of motion of WMR written in a reduced form:

$$\dot{\boldsymbol{q}} = S_1(\boldsymbol{q})\nu + S_2(\boldsymbol{q})\dot{\delta} + S_3(\boldsymbol{q})\dot{\mu} \tag{7}$$

where the velocity vectors of TWMR: $\nu = [\dot{\varphi}_R \quad \dot{\varphi}_L]^T$ and the sliding speed: $\dot{\mu} = [\dot{\mu}_R \quad \dot{\mu}_L]^T$.

So the dynamic equation of the TWMR containing non-holonomic constraints and wheel slippage is:

$$M\dot{\nu} + B\nu + Q\ddot{\mu} + C\dot{\delta} + G\ddot{\delta} + \tau_d = \tau \tag{8}$$

where τ_d represents the external disturbance input.

$$M = S_1^T(\boldsymbol{q})\bar{M}S_1(\boldsymbol{q}) = \begin{bmatrix} m_{11} & m_{12} \\ m_{12} & m_{11} \end{bmatrix}$$

$$B = S_1^T(\boldsymbol{q})\bar{M}\dot{S}_1(\boldsymbol{q}) = m_G\frac{r^2}{2b}\varpi\begin{bmatrix} 0 & 1 \\ -1 & 0 \end{bmatrix}$$

$$Q = S_1^T(\boldsymbol{q})\bar{M}S_3(\boldsymbol{q}) = \begin{bmatrix} q_1 & q_2 \\ q_2 & q_1 \end{bmatrix}$$

$$C = S_1^T(\boldsymbol{q})\bar{M}\dot{S}_2(\boldsymbol{q}) = m_G\frac{r}{2}\varpi\begin{bmatrix} 1 \\ 1 \end{bmatrix}$$

$$G = S_1^T(\boldsymbol{q})\bar{M}S_2(\boldsymbol{q}) = m_G\frac{ar}{2b}\begin{bmatrix} 1 \\ -1 \end{bmatrix}$$

With the coefficients in the matrix:

$$m_{11} = m_G\left(\frac{r^2}{4} + \frac{a^2r^2}{4b^2}\right) + \frac{r^2}{4b^2}(I_G + 2I_D) + 2m_Wr^2 + I_W$$

$$m_{12} = m_G\left(\frac{r^2}{4} - \frac{a^2r^2}{4b^2}\right) - \frac{r^2}{4b^2}(I_G + 2I_D)$$

$$q_1 = m_G\frac{r}{4}\left(1 + \frac{a^2}{b^2}\right) + \frac{r}{4b}(I_G + 2I_D)$$

$$q_2 = m_G\frac{r}{4}\left(1 - \frac{a^2}{b^2}\right) - \frac{r}{4b}(I_G + 2I_D)$$

B. Constructing the Equation of State Describing the Tracking Error of TWMR

Building on the kinematic model (4) and the dynamic model (8) of the TWMR, and accounting for various external disturbances and wheel slippage, we derived the state equations that describe the tracking errors of the TWMR by combining these models. Let the target point T, which follows the specified trajectory, as illustrated in Fig. 1.

The positional discrepancy between point $M(x_M, y_M)$ and the target point $T(x_T, y_T)$ within the coordinate system *MX'Y'* is determined by the following expression [81]:

$$e_p = \begin{bmatrix} e_{p1} \\ e_{p2} \end{bmatrix} = \begin{bmatrix} cos\theta & sin\theta \\ -sin\theta & cos\theta \end{bmatrix}\begin{bmatrix} x_T - x_M \\ y_T - y_M \end{bmatrix} \tag{9}$$

Taking the first time derivative of equation (9), we obtain:

$$\dot{e}_p = \begin{bmatrix} cos\theta & sin\theta \\ -sin\theta & cos\theta \end{bmatrix}\begin{bmatrix} \dot{x}_T \\ \dot{y}_T \end{bmatrix} - \begin{bmatrix} cos\theta & sin\theta \\ -sin\theta & cos\theta \end{bmatrix}\begin{bmatrix} \dot{x}_M \\ \dot{y}_M \end{bmatrix} + \dot{\theta}\begin{bmatrix} e_{p2} \\ e_{p1} \end{bmatrix} \tag{10}$$

The equation governing the motion of the TWMR at point M, considering the impact of wheel slippage, is expressed as [1][58][84]:

$$\begin{cases} \dot{x}_M = \beta cos\theta - \dot{\delta} sin\theta \\ \dot{y}_M = \beta sin\theta + \dot{\delta} cos\theta \\ \dot{\theta} = \varpi \end{cases} \tag{11}$$

So we have the ingredients:

$$\begin{bmatrix} cos\theta & sin\theta \\ -sin\theta & cos\theta \end{bmatrix} \begin{bmatrix} \dot{x}_M \\ \dot{y}_M \end{bmatrix} = \begin{bmatrix} cos\theta & sin\theta \\ -sin\theta & cos\theta \end{bmatrix} \begin{bmatrix} \beta cos\theta - \dot{\delta} sin\theta \\ \beta sin\theta + \dot{\delta} cos\theta \end{bmatrix} = \begin{bmatrix} \beta \\ \dot{\delta} \end{bmatrix} \tag{12}$$

Substitute (2) into (12):

$$\begin{bmatrix} cos\theta & sin\theta \\ -sin\theta & cos\theta \end{bmatrix} \begin{bmatrix} \dot{x}_M \\ \dot{y}_M \end{bmatrix} = \begin{bmatrix} \frac{r(\dot{\varphi}_R + \dot{\varphi}_L)}{2} + \frac{\dot{\mu}_R + \dot{\mu}_L}{2} \\ \dot{\delta} \end{bmatrix} \tag{13}$$

Combining (3), (11) and (13) into (10) we get:

$$\begin{aligned} \dot{e}_p &= \begin{bmatrix} cos\theta & sin\theta \\ -sin\theta & cos\theta \end{bmatrix} \begin{bmatrix} \dot{x}_T \\ \dot{y}_T \end{bmatrix} \\ &+ \begin{bmatrix} \left(\frac{e_{p2}}{b} - 1\right)\frac{r}{2} & -\left(\frac{e_{p2}}{b} + 1\right)\frac{r}{2} \\ -\frac{e_{p1} r}{2b} & \frac{e_{p1} r}{2b} \end{bmatrix} \begin{bmatrix} \dot{\varphi}_R \\ \dot{\varphi}_L \end{bmatrix} \\ &+ \begin{bmatrix} \left(\frac{\dot{\mu}_R - \dot{\mu}_L}{2b}\right) e_{p2} - \frac{\dot{\mu}_R + \dot{\mu}_L}{2} \\ -\left(\frac{\dot{\mu}_R - \dot{\mu}_L}{2b}\right) e_{p1} - \dot{\delta} \end{bmatrix} \end{aligned} \tag{14}$$

$$\Rightarrow \dot{e}_p = \begin{bmatrix} \dot{e}_{p1} \\ \dot{e}_{p2} \end{bmatrix} = \kappa \nu + \xi_1 \tag{15}$$

where: $\kappa = \begin{bmatrix} \left(\frac{e_{p2}}{b} - 1\right)\frac{r}{2} & -\left(\frac{e_{p2}}{b} + 1\right)\frac{r}{2} \\ -\frac{e_{p1} r}{2b} & \frac{e_{p1} r}{2b} \end{bmatrix}$, $\nu = \begin{bmatrix} \dot{\varphi}_R \\ \dot{\varphi}_L \end{bmatrix}$

$$\xi_1 = \begin{bmatrix} \left(\frac{\dot{\mu}_R - \dot{\mu}_L}{2b}\right) e_{p2} - \frac{\dot{\mu}_R + \dot{\mu}_L}{2} \\ -\left(\frac{\dot{\mu}_R - \dot{\mu}_L}{2b}\right) e_{p1} - \dot{\delta} \end{bmatrix} + \begin{bmatrix} cos\theta & sin\theta \\ -sin\theta & cos\theta \end{bmatrix} \begin{bmatrix} \dot{x}_T \\ \dot{y}_T \end{bmatrix}$$

III. CONTROLLER DESIGN FOR TWMR

Let the state variables $x_1 = e_p; x_2 = \dot{x}_1 + \lambda x_1$

where λ is a positive scalar.

The first and second time derivatives of x_1 are obtained as follows:

$$\dot{x}_1 = \dot{e}_p = \kappa \nu + \xi_1 \tag{16}$$

$$\ddot{x}_1 = \kappa \dot{\nu} + \dot{\kappa} \nu + \dot{\xi}_1 \tag{17}$$

Rearranging equation (8), we arrive at (18):

$$\begin{aligned} \dot{\nu} &= -M^{-1} B \nu - M^{-1}\left(Q\ddot{\mu} + C\dot{\delta} + G\ddot{\delta} + \tau_d\right) \\ &\quad + M^{-1}\tau \\ &= -M^{-1} B \nu + M^{-1}\tau + \xi_2 \end{aligned} \tag{18}$$

Where, $\xi_2 = -M^{-1}\left(Q\ddot{\mu} + C\dot{\delta} + G\ddot{\delta} + \tau_d\right)$

Substitute (18) into (17) we get:

$$\ddot{x}_1 = -\kappa M^{-1} B \nu + \kappa M^{-1}\tau + \kappa \xi_2 + \dot{\kappa}\nu + \dot{\xi}_1 \tag{19}$$

The rate of change of x_2 with respect to time is given by:

$$\dot{x}_2 = \ddot{x}_1 + \lambda \dot{x}_1 \tag{20}$$

Substitute (16) and (19) into (20) we get:

$$\begin{aligned} \dot{x}_2 &= \ddot{x}_1 + \lambda \dot{x}_1 \\ &= -\kappa M^{-1} B \nu + \kappa M^{-1}\tau + \kappa \xi_2 + \dot{\kappa}\nu + \dot{\xi}_1 + \lambda \kappa \nu + \lambda \xi_1 \\ &= \mathrm{E}_1 \nu + \mathrm{Z}\tau + \xi_3 \end{aligned} \tag{21}$$

Where, $\mathrm{E}_1 = -\kappa M^{-1} B$, $\mathrm{Z} = \kappa M^{-1}$, $\xi_3 = \kappa \xi_2 + \dot{\kappa}\nu + \dot{\xi}_1 + \lambda \kappa \nu + \lambda \xi_1$.

Rearrangement of equation (16):

$$\begin{aligned} \nu &= \kappa^{-1}\dot{x}_1 - \kappa^{-1}\xi_1 = \kappa^{-1}(x_2 - \lambda x_1) - \kappa^{-1}\xi_1 \\ &= \kappa^{-1} x_2 - \kappa^{-1}\lambda x_1 - \kappa^{-1}\xi_1 \end{aligned} \tag{22}$$

Substitute (22) into (21) we get:

$$\begin{aligned} \dot{x}_2 &= \mathrm{E}_1\kappa^{-1} x_2 - \mathrm{E}_1\kappa^{-1}\lambda x_1 - \mathrm{E}_1\kappa^{-1}\xi_1 + \mathrm{Z}\tau + \xi_3 \\ &= \mathrm{E} x_2 - \lambda \mathrm{E} x_1 + \mathrm{Z}\tau + d \end{aligned} \tag{23}$$

Where, $\mathrm{E} = \mathrm{E}_1\kappa^{-1}$, $d = \xi_3 - \mathrm{E}_1\kappa^{-1}\xi_1$

From this we have the state equation describing the tracking error of the TWMR as (24).

$$\begin{cases} \dot{x}_1 = x_2 - \lambda x_1 \\ \dot{x}_2 = \mathrm{E} x_2 - \lambda \mathrm{E} x_1 + \mathrm{Z}\tau + d \end{cases} \tag{24}$$

Define the sliding surface:

$$s = \vartheta x_1 + x_2 \tag{25}$$

where $\vartheta > 0$.

Substitute $x_2 = \dot{x}_1 + \lambda x_1$ into (25):

$$s = \vartheta x_1 + \dot{x}_1 + \lambda x_1 = (\vartheta + \lambda) x_1 + \dot{x}_1 \tag{26}$$

Choose a Lyapunov function of the following form:

$$V = \frac{1}{2} x_1^2 + \frac{1}{2} s^2 + \frac{1}{2\eta} \tilde{d}^2 \tag{27}$$

where, d is approximated by the adaptive component $\hat{d}$, with the estimation error defined as $\tilde{d} = d - \hat{d}$.

The time derivative of V is given by (28):

$$\dot{V} = x_1\dot{x}_1 + s\dot{s} + \frac{1}{\eta}\tilde{d}\dot{\tilde{d}}$$
$$= x_1(x_2 - \lambda x_1) + s(\vartheta\dot{x}_1 + \dot{x}_2) + \frac{1}{\eta}\tilde{d}\left(\dot{d} - \dot{\hat{d}}\right) \quad (28)$$

$$\Rightarrow \dot{V} = x_1x_2 - \lambda x_1^2$$
$$+s[\vartheta(x_2 - \lambda x_1) + \mathrm{E}x_2 - \lambda\mathrm{E}x_1 + \mathrm{Z}\tau + d] - \frac{1}{\eta}\tilde{d}\dot{\hat{d}} \quad (29)$$

$$\Rightarrow \dot{V} = x_1x_2 - \lambda x_1^2$$
$$+s\left[(\vartheta I + \mathrm{E})x_2 - \lambda(\vartheta I + \mathrm{E})x_1 + \mathrm{Z}\tau + \tilde{d} + \hat{d}\right] \quad (30)$$
$$-\frac{1}{\eta}\tilde{d}\dot{\hat{d}}$$

$$\Rightarrow \dot{V} = x_1x_2 - \lambda x_1^2$$
$$+s\left[(\vartheta I + \mathrm{E})x_2 - \lambda(\vartheta I + \mathrm{E})x_1 + \mathrm{Z}\tau + \hat{d}\right] \quad (31)$$
$$-\frac{1}{\eta}\tilde{d}\left(\dot{\hat{d}} - \eta s\right)$$

where I is the identity matrix.

From equation (31) the controller is selected as follows:

$$\tau = -\mathrm{Z}^{-1}\left[(\vartheta I + \mathrm{E})(x_2 - \lambda x_1) + \hat{d} + ksgn(s)\right] \quad (32)$$

and the adaptive law is:

$$\dot{\hat{d}} = \eta s \quad (33)$$

where k is a positive scalar.

Substituting (32) and (33) into equation (31) we get the following result:

$$\dot{V} = x_1x_2 - \lambda x_1^2 - k|s| \quad (34)$$

Definition of auxiliary variables: $X = \begin{bmatrix}x_1\\x_2\end{bmatrix}$, $\Delta = \begin{bmatrix}\lambda & -2\\1 & 0\end{bmatrix}$

Then do the calculation we have:

$$X^T\Delta X = [x_1 \quad x_2]\begin{bmatrix}\lambda & -2\\1 & 0\end{bmatrix}\begin{bmatrix}x_1\\x_2\end{bmatrix} \quad (35)$$

$$\Rightarrow X^T\Delta X = [\lambda x_1 + x_2 \quad -2x_1]\begin{bmatrix}x_1\\x_2\end{bmatrix}$$
$$= \lambda x_1^2 + x_1x_2 - 2x_1x_2 \quad (36)$$

$$\Rightarrow X^T\Delta X = \lambda x_1^2 - x_1x_2 \quad (37)$$

Comparing (2.25) and (2.28) we have (38):

$$\dot{V}_2 = -X^T\Delta X - k|s| < 0 \quad (38)$$

So the system (24) is closed-loop stable according to the Lyapunov criterion.

The block diagram of the closed loop control system is shown in Fig. 2.

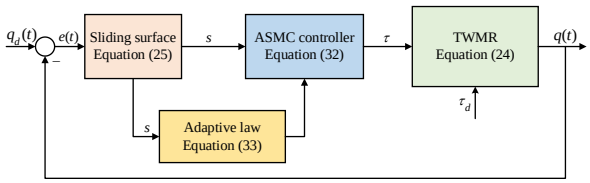

Fig. 2. Block diagram of closed loop control system

IV. Simulation and Experimental Results

A. Simulation Results

In this section, we utilize MATLAB/Simulink to conduct simulations aimed at validating the effectiveness and robustness of the proposed control approach. The simulation setup employs the TWMR model parameters outlined in Table I, conducted under conditions incorporating model uncertainties and external disturbances. Notably, the velocities and accelerations associated with wheel slip are assumed to remain unmeasured. For simplicity and without loss of generality, we consider the following wheel slip dynamics: $[\dot{\mu}_R \quad \dot{\mu}_L \quad \dot{\delta}]^T = [1 + cost \quad 1 + sint \quad cost]^T$ (m/s). Furthermore, the disturbance inputs are characterized as: $\tau_d = [2sin(3t) \quad 2cos(3t)]$ (N.m).

TABLE I. TWMR Parameters [38]

Parameters	Value
Distance between the M and G (a)	0.3 [m]
Inertial moment of the platform (I_G)	15.625 [kgm^2]
Inertial moment of each wheel (Diameter axis - I_D)	0.0025 [kgm^2]
Inertial moment of each wheel (Rotation axis - I_W)	0.1 [kgm^2]
Radius of the wheel (r)	0.15 [m]
Radius of the wheel shaft (b)	0.75 [m]
Weight of each wheel (m_W)	1 [kg]
Weight of the platform (m_G)	30 [kg]

During operation, the parameters of the variation model increased by 25% compared to the initial value, i.e. compared to the standard or previously expected value. This means that the level of variation or error in these parameters increased significantly, making the model more flexible in reflecting actual fluctuations or uncertainties during the TWMR operation.

The controller parameters were carefully adjusted and fine-tuned through trial and error, based on continuous testing and adjustment processes to achieve optimal performance. This process was carried out step by step, based on simulation results, feedback and analysis to adjust the appropriate parameter values, to ensure the controller operates stably and accurately in the system. The final results of this process are clearly presented in Table II, showing the levels of adjustment performed and helping to clarify the process as well as achieve the control performance goals of the system.

TABLE II. Controller Parameters

Parameters	Value
λ	13
η	7
k	20
ϑ	20

In this study, the simulation of the TWMR system operation according to the trifolium reference trajectory was carried out to test the effectiveness of the control method. Specifically, our proposed ASMC controller was compared with the SMC controller presented in the literature [53]. The purpose of this comparison is to clearly demonstrate the superiority of the ASMC control method in improving the accuracy, stability and adaptability of the TWMR system when tracking complex trajectories.

The reference trajectory is expressed by the following equation:

$$\begin{cases} x_T = -t \\ y_T = sin(0{,}5t) + 0{,}5t + 1 \end{cases}$$

Fig. 3 shows the trajectories in a two-dimensional plane, with the x-axis (in meters) and the y-axis (in meters). The solid blue line represents the reference trajectory. The dashed orange line represents the actual trajectory of TWMR using the proposed ASMC controller. Meanwhile, the dashed green line depicts the trajectory when the system is controlled by the SMC method. The initial position of TWMR is $[x_0 \quad y_0 \quad \theta] = [0{,}5 \quad 0 \quad -\pi/4]$. The results show that both controllers achieve good stability, helping the actual trajectory closely follow the expected trajectory. However, the ASMC control helps TWMR approach the target smoothly, while the OSMC control causes initial oscillation, affecting the tracking process. These characteristics are clearly reflected in Fig. 4 and Fig. 5, which show the tracking error on the x-axis and y-axis, respectively.

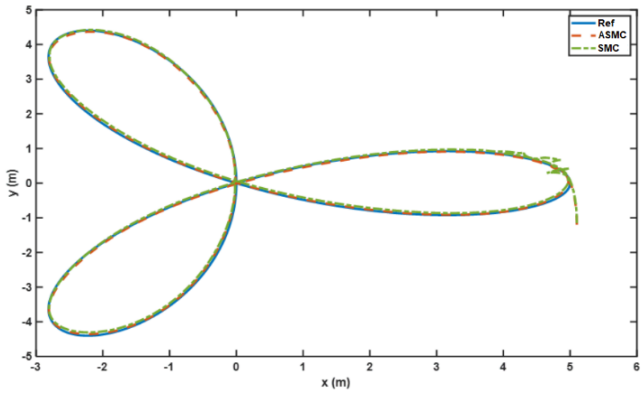

Fig. 3. Comparison of TWMR trajectory tracking using ASMC and SMC

In Fig. 4 and Fig. 5, it is clearly seen that the x- and y-axis deviation errors of the ASMC controller show more stability and smoothness than the oscillation waveform of the SMC controller in the early period, specifically in the first 4 seconds. This difference shows that the system response when using ASMC is quite smooth and has less unwanted oscillations, helping the system to quickly stabilize and follow the desired path more accurately. In contrast, the errors of SMC tend to fluctuate more, causing small fluctuations in the process of catching up with the target, which is especially obvious in the early period of the control process. In addition, the analysis of specific data has been summarized in Table III, which helps to more clearly confirm the performance of these two control methods.

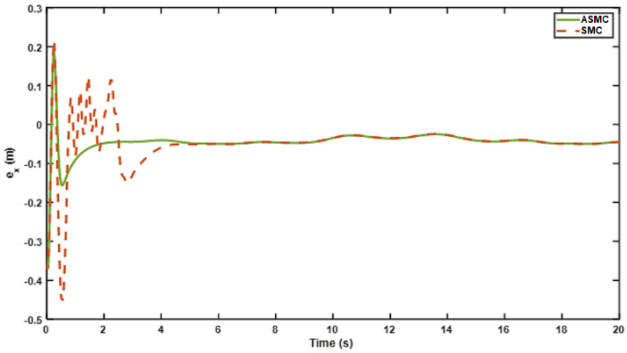

Fig. 4. TWMR x-axis tracking error when using ASMC and SMC

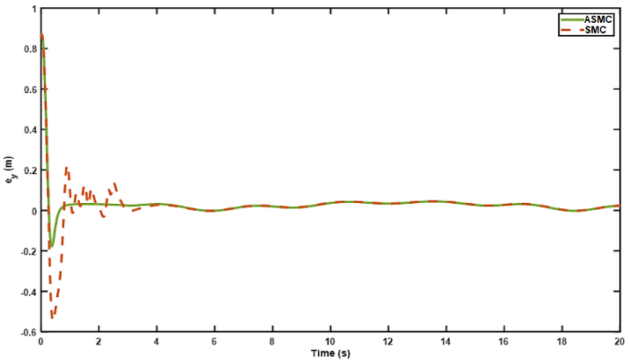

Fig. 5. TWMR x-axis tracking error when using ASMC and SMC

Accordingly, these figures show that the response of ASMC is superior to SMC in response indicators such as accuracy and speed of reaching steady state. In addition, the survey results are also clearly shown in Table III, which reflects that the ASMC controller responds faster and more stably than SMC, contributing to optimizing the system control process. From these figures, it can be concluded that, compared to SMC, ASMC not only helps to reduce errors, increase smoothness in response but also improves the overall controllability of the system, especially in the initial stages when the system just starts to respond.

TABLE III. CONTROLLER PARAMETERS

Controller	Settling time x-axis	Settling time y-axis	Peak error x-axis	Peak error y-axis	MSE x-axis	MSE y-axis
ASMC	2 (s)	0.8 (s)	0.19 (m)	0.19 (m)	0.054	0.145
SMC	5.2 (s)	4 (s)	0.45 (m)	0.54 (m)	0.127	0.258

Then, the system will be programmed to control the TWMR along a different trajectory, specifically a circular path, to test whether the system can adapt and maintain effectiveness across a wider variety of trajectories. This allows us to better assess the capacity and reliability of the TWMR system in real-world applications that require precise movement along various types of paths.

The system is simulated with a circular trajectory as shown in the following equation:

$$\begin{cases} x_T = 5cos(0{,}1\pi t) \\ y_T = 5sin(0{,}1\pi t) \end{cases}$$

The initial position of the TWMR is $[x_0 \quad y_0 \quad \theta] = [6 \quad 0 \quad 0]$. The simulation results are shown in Fig. 6 to Fig. 8.

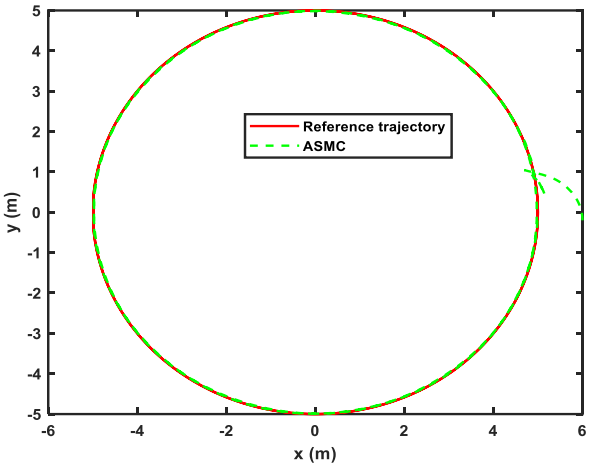

Fig. 6. Circular trajectory tracking TWMR using ASMC method

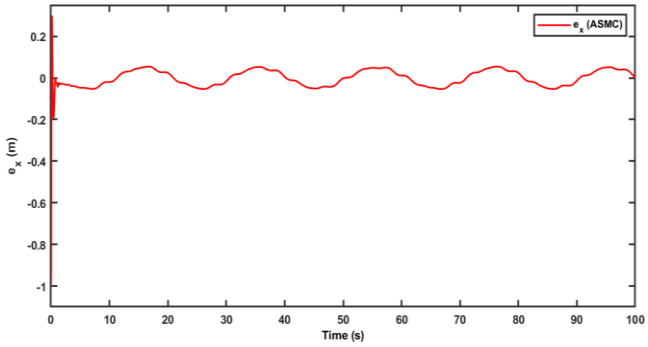

Fig. 7. *x*-axis tracking error using ASMC method

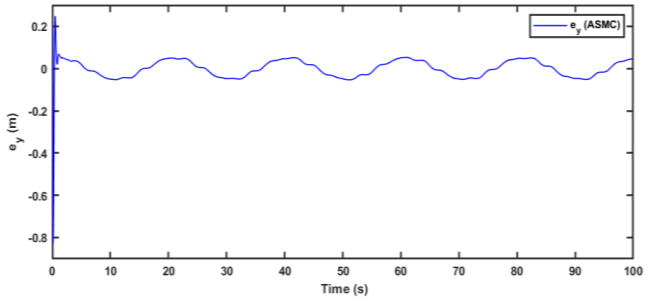

Fig. 8. *y*-axis tracking error using ASMC method

The simulation results in Fig. 6 to Fig. 8 show that the actual trajectory of the WMR starts from the initial position and moves quickly towards the set trajectory and always follows it closely, the transition time is short, the deviation of x, y coordinates is relatively small, fluctuating in the range of -0.07 [m] ÷ 0.07 [m].

B. Experimental Results

After completing the detailed research and analysis of the algorithms through extensive simulation studies conducted on MATLAB-Simulink software, the paper proceeds to present the implementation and experimental validation of these algorithms on the actual TWMR model. This transition from simulation to real-world testing is crucial for verifying the effectiveness, robustness, and practicality of the algorithms under real operating conditions. The experimental run involves implementing the developed control strategies on the TWMR system, closely monitoring its performance in real-time, and comparing the outcomes with the simulation results to assess accuracy and reliability. Such an approach not only demonstrates the feasibility of the algorithms beyond the simulated environment but also provides valuable insights into potential adjustments needed for optimization in practical applications.

The hardware block diagram to build the TWMR system is shown in Fig. 9.

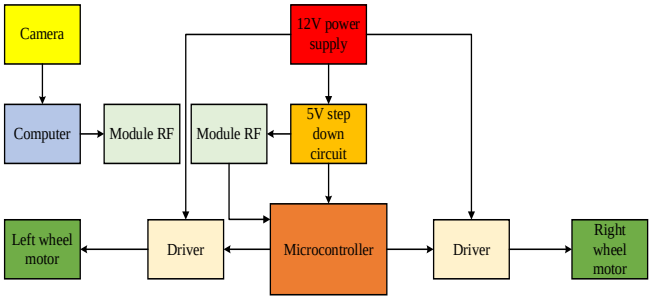

Fig. 9. Hardware block diagram of TWMR system

Fig. 10 shows the TWMR test area installed in the Robotics Engineering Laboratory of the University of Economics – Technology for Industries. We can see that the Robot is placed in a tiled room, the top of the TWMR is covered with red and blue stickers. The purpose of this is to locate the TWMR in space and determine the direction of movement of the TWMR. Above the floor is a Rapoo C260 Camera, when the TWMR moves in the test area, the Camera above will determine the position of the TWMR.

Fig. 10. TWMR test run area

Fig. 11 is the interface on Matlab, showing us the coordinates of TWMR in space, here there is a blue circle, which is the reference trajectory that TWMR must follow. Thanks to this interface, we can observe the TWMR trajectory more easily. To test the ASMC algorithm just designed in the above section, we proceed to run TWMR in practice.

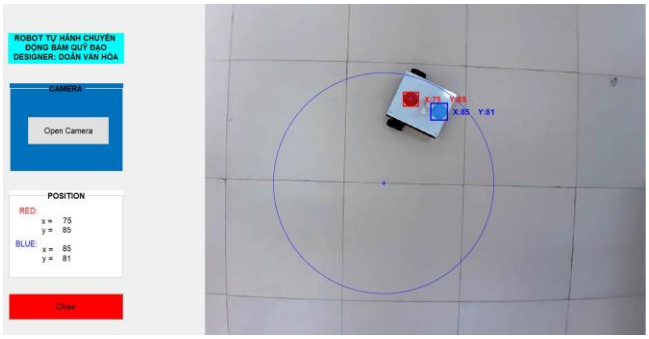

Fig. 11. Monitoring and control interface on Matlab

Fig. 12 shows the trajectory of TWMR moving in a circle with a radius of 40 cm.

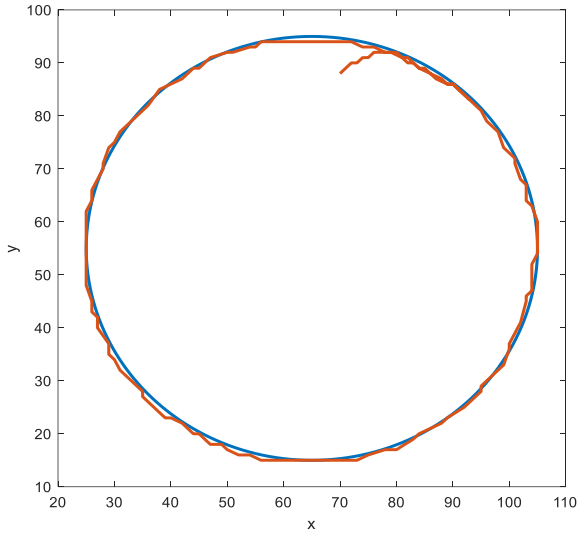

Fig. 12. Experimental results of circular trajectory tracking

The TWMR process actually moves the recorded data. To facilitate the evaluation of the tracking error, the Mean Squared Error (MSE) of TWMR is calculated. The value of MSE is calculated according to the following formula:

$$MSE = \frac{1}{T}\sum_{i=1}^{T}\left(q^i - q_d^i\right)^2 \quad (38)$$

where T is the total number of stored samples, q^i is the actual position and q_d^i is the desired position of the Robot. The results of the MSE values are shown in Table IV.

TABLE IV. MSE OF THE EXPERIMENTALLY MOVING TWMR PROCESS

MSE	Experiment
x	0.25 (cm)
y	0.57 (cm)

Next, the robot is instructed to move along a circular path with a radius of 40 cm. However, in this scenario, a heavy object weighing approximately 0.9 kg is placed on the robot to evaluate its ability to maintain accurate movement under increased load. The results demonstrate that the robot successfully follows the desired trajectory, as illustrated in Fig. 13. Additionally, the MSE values obtained during this test are presented in Table V, providing quantitative measures of the system's tracking accuracy under these conditions.

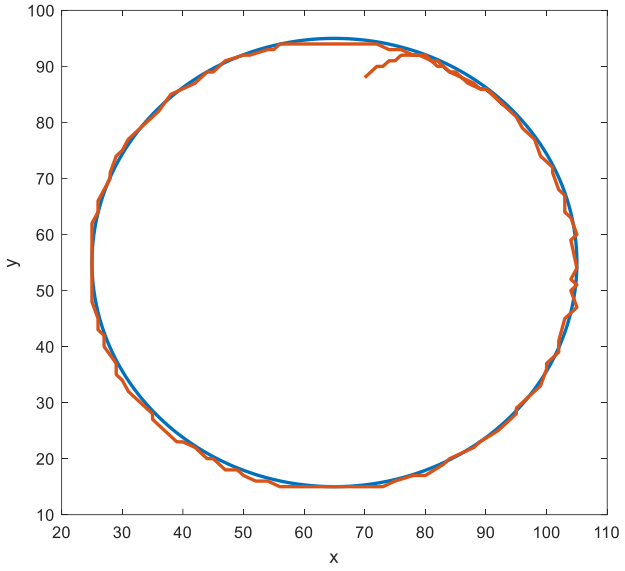

Fig. 13. Experimental results of circular trajectory tracking when carrying additional weight

TABLE V. MSE OF TWMR PROCESS MOVING EXPERIMENTALLY WITH ADDITIONAL LOAD

MSE	Experiment
x	0.28 (cm)
y	0.63 (cm)

TWMR moves along a circular trajectory with a radius of 40 cm for 15 seconds, the trajectory is relatively good and there is deviation (due to mechanical structure). In case the Robot carries additional heavy objects, the Robot still follows the desired trajectory, the deviation is insignificant compared to the case where the Robot has not changed its mass.

V. CONCLUSION AND FUTURE WORK

This study introduces an ASMC approach for precise tracking of a TWMR, accounting for external disturbances and wheel slip effects. The control strategy is built upon a fault state-space representation that combines both kinematic and dynamic models of the system. Disturbances in these models are mitigated through an adaptive law. Compared to earlier research, the proposed control architecture is designed to be more streamlined. Ultimately, simulation and experimental outcomes verify that the controller effectively achieves the desired tracking performance for the TWMR.

The next research focuses on the controller design methods for the state equation model describing the tracking error of TWMR using other control techniques. Extend the results to other actuator-less systems such as self-balancing two-wheeled vehicles, drones, etc. Experimentally deploy different TWMR models in real environments and develop them into commercial products with high practical applications.

ACKNOWLEDGMENT

This study was supported by University of Economics - Technology for Industries, Ha Noi - Vietnam; http://www.uneti.edu.vn/.

REFERENCES

[1] M. Korkmaz, Ö. Aydoğdu, and H. Doğan, "Design and performance comparison of variable parameter nonlinear PID controller and genetic algorithm based PID controller," in *Proc. Int. Symp. Innovations Intell. Syst. Appl. (INISTA)*, pp. 1–5, 2012, doi: 10.1109/INISTA.2012.6246935.

[2] A. Mallem, S. Nourredine, and W. Benaziza, "Mobile robot trajectory tracking using PID fast terminal sliding mode inverse dynamic control," in *Proc. Int. Conf. Control Eng. Inf. Technol. (CEIT)*, pp. 1–6, 2016.

[3] C. S. Shijin and K. Udayakumar, "Speed control of wheeled mobile robots using PID with dynamic and kinematic modelling," in *Proc. Int. Conf. Innovations Inf., Embedded Commun. Syst. (ICIIECS)*, pp. 1–7, 2017.

[4] R. R. Carmona, H. G. Sung, Y. S. Kim, and H. A. Vazquez, "Stable PID control for mobile robots," in *Proc. Int. Conf. Control, Autom., Robot. Vision (ICARCV)*, pp. 1891–1896, 2018.

[5] N. H. Thai, T. T. K. Ly, H. Thien, and L. Q. Dzung, "Trajectory tracking control for differential-drive mobile robot by a variable parameter PID controller," *Int. J. Mech. Eng. Robot. Res.*, vol. 11, no. 8, pp. 614–621, Aug. 2022, doi: 10.18178/ijmerr.11.8.614-621.

[6] N. C. P. and M. S. J., "Robust controller for trajectory tracking of a mobile robot," in *Proc. IEEE Int. Conf. Power Electron., Intell. Control Energy Syst. (ICPEICES)*, pp, 1-6, 2016, doi: 10.1109/ICPEICES.2016.7853137.

[7] S. Roy, S. Nandy, I. N. Kar, R. Ray, and S. N. Shome, "Robust control of nonholonomic wheeled mobile robot with past information: Theory and experiment," *Proc. Inst. Mech. Eng., Part I: J. Syst. Control Eng.*, vol. 231, no. 3, pp. 178–188, 2017, doi: 10.1177/0959651817691641.

[8] A. Abadi *et al.*, "Robust tracking control of wheeled mobile robot based on differential flatness and sliding active disturbance rejection control: Simulations and experiments," *Sensors*, vol. 24, no. 9, p. 2849, 2024.

[9] A. Andreev and O. Peregudova, "On the trajectory tracking control of a wheeled mobile robot based on a dynamic model with slip," in *Proc. Int. Conf. Stability Oscillations Nonlinear Control Syst. (STAB)*, pp. 1–4, 2020, doi: 10.1109/STAB49150.2020.9140714.

[10] H. V. Doan and N. T.-T. Vu, "Adaptive sliding mode control for uncertain wheel mobile robot," *Int. J. Electr. Comput. Eng. (IJECE)*, vol. 13, no. 4, pp. 3939–3947, Aug. 2023.

[11] M. Cui, "Observer-based adaptive tracking control of wheeled mobile robots with unknown slipping parameters," *IEEE Access*, vol. 7, pp. 169646–169655, 2019.

[12] L. Yan, B. Ma, Y. Jia, and Y. Jia, "Observer-based trajectory tracking control of nonholonomic wheeled mobile robots," *IEEE Trans. Control Syst. Technol.*, vol. 32, no. 3, pp. 1114–1121, 2024.

[13] D. Wang, S. Pan, J. Zhou, Q. Pan, Z. Miao, and J. Yang, "Event-triggered integral formation controller for networked nonholonomic mobile robots: Theory and experiment," *IEEE Trans. Intell. Transp. Syst.*, vol. 24, no. 12, pp. 14620–14632, 2023.

[14] D. Wang, J. Zhou, C. He, and Z. Miao, "Experimental verification of formation control in nonholonomic multi-mobile robots," in *Proc. Chin. Control Conf. (CCC)*, pp. 5327–5331, 2021.

[15] G. Xue, Z. Ding, Q. Zhang, Y. Liu, Y. Hu, and Z. Tao, "Trajectory tracking control of tracked underwater dredging robot," in *Proc. Int. Conf. Control Robot. Eng. (ICCRE)*, pp. 81–85, 2021.

[16] C. M. Sanchez, V. M. Hernández-Guzmán, R. Silva-Ortigoza, M. Antonio-Cruz, and C. A. Merlo-Zapata, "Intuitive planning, generation, and tracking of trajectory for WMR with mobile computing device and embedded system," *IEEE Access*, vol. 8, pp. 160627–160642, 2020.

[17] M. Vazquez, M. Ardito-Proulx, and S. Wadoo, "Lyapunov based trajectory tracking dynamic control for a QBOT-2," in *Proc. IEEE Integr. STEM Educ. Conf. (ISEC)*, pp. 1–6, 2020.

[18] M. R. Febsya, R. Ardhi, A. Widyotriatmo, and Y. Y. Nazaruddin, "Design control of forward motion of an autonomous truck-trailer using Lyapunov stability approach," in *Proc. Int. Conf. Instrum., Control, Autom. (ICA)*, pp. 65–70, 2019.

[19] A. Dun, R. Wang, Q. Xu, and J. Zhai, "Leader-follower formation control of multiple wheeled mobile robot systems based on dynamic surface control," in *Proc. Chin. Autom. Congr. (CAC)*, pp. 5357–5361, 2020.

[20] W. M. Nikshi, R. C. Hoover, M. D. Bedillion, and S. Shahmiri, "Trajectory tracking of the mixed conventional/braking actuation mobile robots using model predictive control," in *Proc. IEEE Int. Conf. Control Autom. (ICCA)*, pp. 704–709, 2018.

[21] C. U. Dogruer, "Trajectory tracking control of a mobile robot with model predictive controller and observer," in *Proc. Int. Conf. Control, Mechatronics Autom. (ICCMA)*, pp. 179–184, 2019.

[22] Y. Zhang, X. Zhao, B. Tao, and H. Ding, "Point stabilization of nonholonomic mobile robot by Bézier smooth subline constraint nonlinear model predictive control," *IEEE/ASME Trans. Mechatronics*, vol. 26, no. 2, pp. 990–1001, 2021.

[23] R. Hedjar, "Approximate quadratic programming algorithm for nonlinear model predictive tracking control of a wheeled mobile robot," *IEEE Access*, vol. 10, pp. 65067–65079, 2022.

[24] N. S. Tran, K. L. Lai, and P. N. Dao, "A novel model predictive control for an autonomous four-wheel independent vehicle," *Int. J. Mech. Eng. Robot. Res.*, vol. 13, no. 5, pp. 509–515, 2024.

[25] C.-H. Sun, Y.-T. Wang, and C.-C. Chang, "Design of T-S fuzzy controller for two-wheeled mobile robot," in *Proc. Int. Conf. Syst. Sci. Eng. (ICSSE)*, 2011, doi: 10.1109/ICSSE.2011.5961903.

[26] M.-C. Kao, C.-J. Lin, C.-L. Feng, T.-H. S. Li, and H.-M. Yen, "Adaptive type-2 fuzzy tracking control of wheeled mobile robots," in *Proc. Int. Conf. Fuzzy Theory Appl. (iFUZZY)*, 2013, doi: 10.1109/iFUZZY.2013.6825400.

[27] Q. Xu, J. Kan, S. Chen, and S. Yan, "Fuzzy PID based trajectory tracking control of mobile robot and its simulation in Simulink," *Int. J. Control Autom.*, vol. 7, no. 8, pp. 233–244, 2014, doi: 10.14257/ijca.2014.7.8.20.

[28] N. Hacene and B. Mendil, "Fuzzy behavior-based control of three wheeled omnidirectional mobile robot," *Int. J. Autom. Comput.*, vol. 16, pp. 163-185, 2018, doi: 10.1007/s11633-018-1135-x.

[29] R. Morales, J. A. Somolinos, C. E. Ugalde-Loo, and J. Gaspar, "Robotics and control engineering of wave and tidal energy-recovering systems," *Math. Probl. Eng.*, vol. 2018, pp. 1–2, 2018, doi: 10.1155/2018/6594517.

[30] M. Abdelwahab, V. Parque, A. M. R. Fath Elbab, A. A. Abouelsoud, and S. Sugano, "Trajectory tracking of wheeled mobile robots using Z-number based fuzzy logic," *IEEE Access*, vol. 8, pp. 18426–18441, 2020, doi: 10.1109/ACCESS.2020.2968421.

[31] A. Štefek, V. T. Pham, V. Krivanek, and K. L. Pham, "Optimization of fuzzy logic controller used for a differential drive wheeled mobile robot," *Appl. Sci.*, vol. 11, no. 13, p. 6023, 2021, doi: 10.3390/app11136023.

[32] Z. Li, J. Deng, R. Lu, Y. Xu, J. Bai, and C.-Y. Su, "Trajectory-tracking control of mobile robot systems incorporating neural-dynamic optimized model predictive approach," *IEEE Trans. Syst., Man, Cybern.: Syst.*, vol. 46, no. 6, pp. 740–749, 2016, doi: 10.1109/TSMC.2015.2465352.

[33] P. Bozek, Y. L. Karavaev, A. A. Ardentov, and K. S. Yefremov, "Neural network control of a wheeled mobile robot based on optimal trajectories," *Int. J. Adv. Robot. Syst.*, vol. 17, no. 2, 2020, doi: 10.1177/1729881420916077.

[34] D. Trujillo, L. A. Morales, D. Chávez, and D. F. Pozo, "Trajectory tracking control of a mobile robot using neural networks," *Emerg. Sci. J.*, vol. 7, no. 6, pp. 1843–1862, Dec. 2023, doi: 10.28991/ESJ-2023-07-06-01.

[35] C. Chaodaa, J. Nie, T. Zhang, Z. Li, L. Shan, and Z. Huang, "Trajectory tracking control of super-twisting sliding mode of mobile robot based on neural network," *J. Comput. Methods Sci. Eng.*, vol. 23, no. 1, pp. 101–115, 2023, doi: 10.3233/JCM-226507.

[36] T. T. K. Ly, N. T. Thanh, H. Thien, and T. Nguyen, "A neural network controller design for the Mecanum wheel mobile robot," *Eng., Technol. Appl. Sci. Res.*, vol. 13, no. 2, pp. 10541–10547, Apr. 2023, doi: 10.48084/etasr.5761.

[37] D. V. Hoa, T. D. Chuyen, L. K. Lai, and L. T. T. Ha, "Trajectory tracking control for wheeled mobile robot system with uncertain nonlinear model based on integral reinforcement learning algorithm," *Int. J. Eng. Trends Technol.*, vol. 72, no. 5, pp. 290–298, May 2024.

[38] H. V. Doan and N. T.-T. Vu, "Robust optimal control for uncertain wheeled mobile robot based on reinforcement learning: ADP approach," *Bull. Electr. Eng. Inform.*, vol. 13, no. 3, pp. 1524–1534, Jun. 2024.

[39] C. Zeng, A. Su, T. Chen, and S. Z. Chen, "Observer-based adaptive neural network control: the convergence properties analysis under the influence of persistent excitation level," *Nonlinear Dyn.*, pp. 1-17, 2024, doi: 10.1007/s11071-024-10521-1.

[40] P. Liang and W. Yuan, "Design of intelligent remote control car based on MCU," in *Proc. Int. Conf. Inf. Technol. Med. Educ. (ITME)*, pp. 206–209, 2022.

[41] A. Moran and M. Nagai, "Autonomous driving of truck-trailer mobile robots with linear-fuzzy control for trajectory following," in *Proc. IEEE Int. Conf. Fuzzy Syst. (FUZZ-IEEE)*, pp. 1–8, 2020.

[42] J. Qiao, "Research on motion modeling and control of tracking car based on neural network," in *Proc. Int. Conf. Comput. Data Sci. (CDS)*, pp. 282–286, 2021.

[43] R. Euldji *et al*., "Optimal backstepping-FOPID controller design for wheeled mobile robot," *J. Eur. Syst. Automatisés*, vol. 55, no. 1, pp. 97–107, Feb. 2022.

[44] J. Bai, Z. Yang, Z. Li, C. Shen, Y. Chen, and J. Li, "Trajectory tracking controller design for wheeled mobile robot with velocity and torque constraints," *Int. J. Syst. Sci.*, vol. 55, no. 14, pp. 2825–2837, 2024, doi: 10.1080/00207721.2024.2354844.

[45] X. Shen and W. Shi, "Adaptive trajectory tracking control of wheeled mobile robot," in *Proc. Chin. Control Decis. Conf. (CCDC)*, pp. 5161–5165, 2019, doi: 10.1109/CCDC.2019.8833019.

[46] H. Ye and S. Wang, "Trajectory tracking control for nonholonomic wheeled mobile robots with external disturbances and parameter uncertainties," *Int. J. Control Autom. Syst.*, vol. 18, no. 12, pp. 3015-3022, 2020, doi: 10.1007/s12555-019-0643-y.

[47] Q. Liu and Q. Cong, "Kinematic and dynamic control model of wheeled mobile robot under internet of things and neural network," *J. Supercomput.*, vol. 78, pp. 8678–8707, 2022, doi: 10.1007/s11227-021-04160-1.

[48] B. Chai, K. Zhang, and M. Tan, "Optimized trajectory tracking control with disturbance resistance for wheeled mobile robot," *Trans. Inst. Meas. Control*, 2024, doi: 10.1177/01423312241283522.

[49] D. Luo, Y. Huang, X. Huang, M. Miao, and X. Gao, "Active disturbance rejection trajectory tracking control for inspection mobile robots," in *Proc. IEEE Int. Conf. Mechatronics Autom. (ICMA)*, pp. 1366–1371, 2024, doi: 10.1109/ICMA61710.2024.10632938.

[50] K. Byeon, S. You, Y. Lee, S. Kim, D. Kang, J. Choi, and W. Kim, "Robust arbitrary-time path-tracking control using reduced order kinematic model for unmanned ground vehicles," *IEEE Trans. Intell. Transp. Syst.*, vol. 25, no. 5, pp. 4089–4101, 2024.

[51] L. Yang and S. Pan, "A sliding mode control method for trajectory tracking control of wheeled mobile robot," *J. Phys.: Conf. Ser.*, vol. 1074, p. 012059, 2018.

[52] N. K. Goswami and P. K. Padhy, "Sliding mode controller design for trajectory tracking of a non-holonomic mobile robot with disturbance," *Comput. Electr. Eng.*, vol. 72, pp. 307–323, 2018.

[53] K. Alipour, A. B. Robat, and B. Tarvirdizadeh, "Dynamics modeling and sliding mode control of tractor-trailer wheeled mobile robots subject to wheels slip," *Mech. Mach. Theory*, vol. 138, pp. 16–37, 2019.

[54] Y. Zheng, J. Zheng, K. Shao, H. Zhao, H. Xie, and H. Wang, "Adaptive trajectory tracking control for nonholonomic wheeled mobile robots: A barrier function sliding mode approach," *IEEE/CAA J. Autom. Sinica*, vol. 11, no. 4, pp. 1007–1021, Apr. 2024, doi: 10.1109/JAS.2023.124002.

[55] Y. Li, et al., "Simultaneous tracking and stabilization of nonholonomic wheeled mobile robots under constrained velocity and torque," *Mathematics*, vol. 12, no. 13, pp. 1–17, Jun. 2024, doi: 10.3390/math12131985.

[56] K. L. Fetzer, S. Nersesov, and H. Ashrafiuon, "Sliding mode control of underactuated vehicles in three-dimensional space," in *Proc. Annu. Amer. Control Conf. (ACC)*, pp. 5344–5349, 2018.

[57] S. Peng and W. Shi, "Time-varying sliding mode control of a nonholonomic wheeled mobile robot," in *Proc. Chin. Control Decis. Conf. (CCDC)*, pp. 3140–3145, 2018.

[58] X. Wu, P. Jin, T. Zou, Z. Qi, H. Xiao, and P. Lou, "Backstepping trajectory tracking based on fuzzy sliding mode control for differential mobile robots," *J. Intell. Robot. Syst.*, vol. 96, no. 4, pp. 109–121, 2019.

[59] T. T. Pham, M. Thanh, and C.-N. Nguyen, "Omnidirectional mobile robot trajectory tracking control with diversity of inputs," *Int. J. Mech. Eng. Robot. Res.*, vol. 10, no. 11, 2021.

[60] Z. Xu, S. X. Yang, and S. A. Gadsden, "Enhanced bioinspired backstepping control for a mobile robot with unscented Kalman filter," *IEEE Access*, vol. 8, pp. 125899–125908, 2020, doi: 10.1109/ACCESS.2020.3007881.

[61] S. Fadlo, A. A. Elmahjoub, and N. Rabbah, "Optimal trajectory tracking control for a wheeled mobile robot using backstepping technique," *Int. J. Electr. Comput. Eng. (IJECE)*, vol. 12, no. 6, pp. 5979-5987, 2022.

[62] M. J. Rabbani and A. Y. Memon, "Output feedback stabilization of nonholonomic wheeled mobile robot using backstepping control," in *Proc. IEEE Int. Conf. Control Syst., Comput. Eng. (ICCSCE)*, pp. 119–124, 2022.

[63] U. Ahmad, Y.-J. Pan, H. Shen, and S. Liu, "Cooperative control of mobile manipulators transporting an object based on an adaptive backstepping approach," in *Proc. IEEE Int. Conf. Control Autom. (ICCA)*, pp. 198–203, 2018.

[64] Y. Chen, F. Xue, X. Su, and S. Wang, "Adaptive-sliding-mode disturbance-observer-based control for mobile wheeled robot system," in *Proc. Chin. Control Decis. Conf. (CCDC)*, pp. 3442–3446, 2023.

[65] Z. Chen, D. Liao, and A. Y. Krasnov, "Adaptive control of an uncertain differential drive robot," in *Proc. Int. Conf. Control Sci. Syst. Eng. (ICCSSE)*, pp. 100–104, 2022.

[66] Z. Zhang, W. Jiang, and S. S. Ge, "Adaptive tracking control of nonholonomic mobile robots with input constraints and unknown disturbance," in *Proc. Asian Control Conf. (ASCC)*, pp. 396–402, 2022.

[67] B. Moudoud, H. Aissaoui, and M. Diany, "Finite-time adaptive trajectory tracking control based on sliding mode for wheeled mobile robot," in *Proc. Int. Multi-Conf. Syst., Signals Devices (SSD)*, pp. 1148–1153, 2021.

[68] Y. Ma, B. Jiang, and V. Cocquempot, "Modeling and adaptive fault compensation for two physically linked 2WD mobile robots," *IEEE/ASME Trans. Mechatronics*, vol. 26, no. 2, pp. 1161–1171, 2021.

[69] B. Moudoud, H. Aissaoui, and M. Diany, "Robust trajectory tracking control based on sliding mode of differential driving four-wheeled mobile robot," in *Proc. IEEE Int. Conf. Optimization Appl. (ICOA)*, pp. 1–5, 2020.

[70] J.-X. Zhang, J. Ding, and T. Chai, "Fault-tolerant prescribed performance control of wheeled mobile robots: A mixed-gain adaption approach," *IEEE Trans. Autom. Control*, vol. 69, no. 8, pp. 5500–5507, 2024.

[71] J.-W. Li, "Adaptive tracking and stabilization of nonholonomic mobile robots with input saturation," *IEEE Trans. Autom. Control*, vol. 67, no. 11, pp. 6173–6179, 2022.

[72] S.-L. Dai, K. Lu, and J. Fu, "Adaptive finite-time tracking control of nonholonomic multirobot formation systems with limited field-of-view sensors," *IEEE Trans. Cybern.*, vol. 52, no. 10, pp. 10695–10708, 2022.

[73] H. Long, Q. Wang, J. Zhao, and T. Guo, "Auxiliary variable based adaptive sliding-mode control for systems with mismatched disturbances," in *Proc. Int. Conf. Comput. Eng. Intell. Control (ICCEIC)*, pp. 253–257, 2020.

[74] N. V. Lanh, D. H. Kim, S. K. Jeong, C. H. Lee, H. K. Kim, and S. B. Kim, "Trajectory tracking controller design for caterpillar vehicles using a model reference adaptive controller," in *Proc. Int. Conf. Control, Autom. Syst. (ICCAS)*, pp. 1046–1053, 2020.

[75] W. Sun, S.-F. Su, J. Xia, and Y. Wu, "Adaptive tracking control of wheeled inverted pendulums with periodic disturbances," *IEEE Trans. Cybern.*, vol. 50, no. 5, pp. 1867–1876, 2020.

[76] M. Shirzadeh, M. H. Shojaeefard, A. Amirkhani, and H. Behroozi, "Adaptive fuzzy nonlinear sliding-mode controller for a car-like robot," in *Proc. Conf. Knowl. Based Eng. Innov. (KBEI)*, pp. 686–691, 2019.

[77] S. Peng and W. Shi, "Adaptive fuzzy output feedback control of a nonholonomic wheeled mobile robot," *IEEE Access*, vol. 6, pp. 43414–43424, 2018.

[78] W. Ding, J.-X. Zhang, and P. Shi, "Adaptive fuzzy control of wheeled mobile robots with prescribed trajectory tracking performance," *IEEE Trans. Fuzzy Syst.*, vol. 32, no. 8, pp. 4510–4521, 2024.

[79] Y.-H. Jing and G.-H. Yang, "Adaptive fuzzy output feedback fault-tolerant compensation for uncertain nonlinear systems with infinite number of time-varying actuator failures and full-state constraints," *IEEE Trans. Cybern.*, vol. 51, no. 2, pp. 568–578, 2021.

[80] D. Chwa and J. Boo, "Adaptive fuzzy output feedback simultaneous posture stabilization and tracking control of wheeled mobile robots with kinematic and dynamic disturbances," *IEEE Access*, vol. 8, pp. 228863–228878, 2020.

[81] Y.-H. Jing and G.-H. Yang, "Fuzzy adaptive fault-tolerant control for uncertain nonlinear systems with unknown dead-zone and unmodeled dynamics," *IEEE Trans. Fuzzy Syst.*, vol. 27, no. 12, pp. 2265–2278, 2019.

[82] Z. Chen, Y. Liu, W. He, H. Qiao, and H. Ji, "Adaptive-neural-network-based trajectory tracking control for a nonholonomic wheeled mobile robot with velocity constraints," *IEEE Trans. Ind. Electron.*, vol. 68, no. 6, pp. 5057–5067, 2021, doi: 10.1109/TIE.2020.2989711.

[83] P. Zhang, J. Zhang, and Z. Zhang, "Design of RBFNN-based adaptive sliding mode control strategy for active rehabilitation robot," *IEEE Access*, vol. 8, pp. 155538–155547, Aug. 2020.

[84] T. Zheng, A. Yang, M. Wang, M. Huang, and B. Rao, "Neural network-based adaptive tracking control of mobile robots in the presence of modelling error and disturbances," in *Proc. 34th Chinese Control Conf. (CCC)*, pp. 3173–3178, 2015.

[85] Q. Zhou, S. Zhao, H. Li, R. Lu, and C. Wu, "Adaptive neural network tracking control for robotic manipulators with dead zone," *IEEE Trans. Neural Netw. Learn. Syst.*, vol. 30, no. 12, pp. 3611–3620, 2019.

[86] N. T.-T. Vu, L. X. Ong, N. H. Trinh, and S. T. H. Pham, "Robust adaptive controller for wheel mobile robot with disturbances and wheel slips," *Int. J. Electr. Comput. Eng.*, vol. 11, pp. 336–346, 2021, doi: 10.11591/ijece.v11i1.pp336-346.

[87] V. Q. Ha, S. T. H. Pham, and N. T.-T. Vu, "Adaptive fuzzy type-2 controller for wheeled mobile robot with disturbances and wheelslips," *J. Robot.*, 2021, doi: 10.1155/2021/6946210.

[88] S. J. Yoo, "Adaptive tracking and obstacle avoidance for a class of mobile robots in the presence of unknown skidding and slipping," *IET Control Theory Appl.*, vol. 5, no. 14, pp. 1597–1608, 2011.

[89] T. Nguyen and L. Le, "Neural network-based adaptive tracking control for a nonholonomic wheeled mobile robot with unknown wheel slips, model uncertainties, and unknown bounded disturbances," *Turk. J. Electr. Eng. Comput. Sci.*, vol. 26, no. 1, pp. 378–392, 2018.

[90] T. Nguyen, T. Hoang, M. Pham, and N. Dao, "A Gaussian wavelet network-based robust adaptive tracking controller for a wheeled mobile robot with unknown wheel slips," *International Journal of Control*, vol. 92, no. 11, pp. 2681–2692, 2019.

[91] S. Li, L. Ding, H. Gao, C. Chen, Z. Liu, and Z. Deng, "Adaptive neural network tracking control-based reinforcement learning for wheeled mobile robots with skidding and slipping," *Neurocomputing*, vol. 283, pp. 20–30, 2018.

[92] W. Li, J. Guo, L. Ding, J. Wang, H. Gao, and Z. Deng, "Teleoperation of wheeled mobile robot with dynamic longitudinal slippage," *IEEE Transactions on Control Systems Technology*, vol. 31, no. 1, pp. 99–113, 2023.

[93] W. Li, S. Liu, D. Ren, J. Wang, and H. Gao, "Bilateral teleoperation of wheeled mobile robots subject to lateral sliding on soft terrains," in *Proc. 39th Chinese Control Conf. (CCC)*, 2020, pp. 2697–2702.

[94] R. M. Colorado, J. A. R. Arellano, and L. Aguilar, "Observer-based finite-time control of perturbed wheeled mobile robots," *Authorea Preprints*, 2023, doi: 10.36227/techrxiv.24130800.v1.

[95] J. Bai *et al.*, "Trajectory tracking control for wheeled mobile robots with kinematic parameter uncertainty," *International Journal of Control, Automation and Systems*, vol. 20, pp. 1632–1639, 2022, doi: 10.1007/s12555-021-0212-z.

[96] A. Saldivar-Mendez, J. Gomez-Casas, and A. Morales-Diaz, "Data-driven kinematic control with adaptive gains for a redundant robot," in *Proc. 21st Int. Conf. on Electrical Engineering, Computing Science and Automatic Control (CCE)*, pp. 1–6, 2024.

[97] M. Vazquez, M. Ardito-Proulx, and S. Wadoo, "Nonlinear kinematic control of QBot2-trajectory tracking," in *Proc. IEEE MIT Undergraduate Research Technology Conf. (URTC)*, pp. 1–4, 2019.